ELSEVIER

Int. J. Miner. Process. 65 (2002) 83–108

INTERNATIONAL JOURNAL OF MINERAL PROCESSING

www.elsevier.com/locate/ijminpro

Characterization of a natural and an electro-oxidized arsenopyrite: a study on electrochemical and X-ray photoelectron spectroscopy

M.C. Costa [a,*], A.M. Botelho do Rego [b,1], L.M. Abrantes [c,2]

[a] *Faculdade de Engenharia de Recursos Naturais, FERN, Universidade do Algarve, Campus Universitário de Gambelas, 8000-117 Faro, Portugal*

[b] *Centro de Química-Física Molecular, Complexo Interdisciplinar, IST, Av. Rovisco Pais, 1049-001 Lisbon, Portugal*

[c] *Departamento de Química e Bioquímica, Faculdade de Ciências, Universidade de Lisboa, Rua Ernesto de Vasconcelos, Bloco C8, 3°Piso, 1749-016 Lisbon, Portugal*

Received 5 March 1999; accepted 11 June 2001

Abstract

This paper discusses the results of a detailed study on the electrochemistry of an arsenopyrite mineral and a concentrate as well as other mineral species contained in it in a chloride medium (NaCl 1.9 M + HCl 0.1 M) using cyclic voltammetry.

The surface modification promoted by the anodic oxidation of arsenopyrite mineral samples (+0.8 V for 1 h) is also analysed. X-ray photoelectron spectroscopy (XPS) and Raman spectroscopy have been used to provide information on the chemical state of natural and electro-oxidized surfaces. The results showed that layers of elemental sulphur are produced on the oxidized surface of arsenopyrite by the formation of an intermediate metal-deficient sulphide $Fe_{1-x}As_{1-y}S$. Other surface oxidation products such as iron oxides, arsenic oxides and oxy-sulphur species have also been detected, confirming the interpretation of the voltammetric studies. The identified surface products show that arsenopyrite oxidation occurs by the diffusion of the metal atoms from the bulk to the interface region and by their interaction with air forming metal oxide layers (mainly iron and arsenic oxides) and leaving a predominant elemental sulphur layer.

* Corresponding author. Fax: +351-2-8981-5927.

E-mail addresses: mcorada@ualg.pt (M.C. Costa), amrego@ist.utl.pt (A.M. Botelho do Rego), luisa.abrantes@cd.fc.ul.pt (L.M. Abrantes).

[1] Fax: +351-2-1846-4455/7.

[2] Fax: +351-2-1750-0088.

PII: S0301-7516(01)00059-X

XPS intensity ratios yielded mineral surface stoichiometry before and after electrochemical treatment. Based on the fitted XPS spectra new data for the binding energies of core electrons in arsenopyrite are proposed: 707.3 eV for the Fe $2p_{3/2}$ level, 162.3 eV for the S $2p_{3/2}$ level and 41.5 eV for the As $3d_{5/2}$ level.

The effect that electrochemical pre-treatment of refractory arsenopyrite concentrate has towards the breakdown of the sulphide matrix required for the release of the occluded gold is also discussed, taking into account the results obtained in this study.

Keywords: Arsenopyrite; Electro-oxidation; X-ray photoelectron spectroscopy; Raman spectroscopy

1. Introduction

The growing worldwide demand for gold and the depletion of the high-grade deposits have made complex sulphide ores an increasingly important source of precious metals (Santos et al., 1993; Paterson, 1990). It is well known that these ores usually contain gold in association with arsenopyrite (Prasad et al., 1991; Woods et al., 1989), therefore granting them a significant economic importance. However, most of the gold is often found as very finely disseminated particles inside the mineral layer, thus inaccessible to the leaching agent. To achieve an acceptable recovery of gold from such ores, pre-treatment is required in order to break down the sulphide matrix and render the gold amenable to be recovered, before applying any conventional treatment.

Roasting before cyanide leaching has traditionally been used to process refractory sulphide ores (McCliney, 1990). Nevertheless, several environment restrictions have led to the development of alternative pre-treatments and different approaches, including chemical and bacterial oxidation have been considered. (Frutos, 1998; Dunn and Chamberlain, 1997; Goode, 1993; Fleming, 1992; Attia and El-Kezy, 1989; Kontopoulos and Stefanakis, 1989). The disadvantages of cyanidation—low kinetics and high toxicity of the solutions—have also encouraged research of other leaching systems (Deschênes et al., 1998; Murthy and Prasad, 1996; Ahgelidis and Kydros, 1995; Iglesias et al., 1993; Zipperian et al., 1988). The use of thiourea solutions is reported as being particularly successful (Lacoste-Bouchet et al., 1998; Ubaldini et al., 1998; Tremblay et al., 1996; Bruckard et al., 1993).

The extraction of gold from an arsenopyritic concentrate exhibiting refractory behaviour proved that electro-oxidation can be a potential alternative pre-treatment (Abrantes and Costa, 1996; Costa, 1996). In fact, the application of an anodic potential in a chloride acidic solution considerably improved the subsequent response of the raw material to the hydrometallurgical treatment. After acid thiourea leaching of the electroreacted residue, almost all the gold was extracted, while by direct leaching only a small percentage was extracted.

Therefore, the study of the surface transformation during anodic oxidation of arsenopyrite is important to understand the mechanism that leads to the release of the precious metal occluded in the sulphide matrix. However, electrochemical characterization of surfaces lacks the molecular specificity required to unequivocally identify the species formed on mineral surfaces. For this reason spectroscopic techniques, which provide

information on the elemental and molecular composition of surfaces, have been increasingly used (Marabini et al., 1993; Mernagh and Trudu, 1993; Woods, 1992; McCarron et al., 1990). X-ray photoelectron spectroscopy (also called electron spectroscopy for chemical analysis, ESCA) is particularly appropriate for the study of mineral surfaces since knowledge of the chemical environment of atoms is usually required in addition to elemental composition. Due to its excellent surface sensitivity—of approximately 20 to 30 Å in thickness (Briggs and Seah, 1996)—this technique is an important tool to provide chemical state information about altered and unaltered surfaces. Such information is relevant for the identification of the surface oxidation of mineral sulphides, since, for example, different sulphur compounds need to be distinguished from each other and from the sulphur present in the mineral itself. An X-ray photoelectron is ejected as a result of bombardment with X-radiation. The core electrons are emitted with quantified kinetic energies that can be related with the binding energies (BE), which are characteristic of the chemical phases present in the material.

In recent times spectroscopic techniques such as X-ray photoelectron spectroscopy (XPS) and Raman spectroscopy are becoming frequently used to identify surface compounds on minerals, since surface properties play an important role in many aspects of mineral processing (Mielczarski et al., 1996a,b; Turcotte et al., 1993; Buckley and Woods, 1984). Thus, much research has been carried out on sulphides other than arsenopyrite, whose chemistry in relation to leaching, flotation and its electrochemistry in particular, has received little attention. In fact, in contrast with pyrite relatively few studies have been devoted to the surface analysis of arsenopyrite. Among them, the first steps of surface oxidation have been the subject of a few papers, mainly devoted to arsenopyrite oxidation in alkaline media aimed at a better understanding about the phenomena, controlling mineral response to flotation (Wang et al., 1992; Richardson and Vaughan, 1989; Beattie and Poling, 1987). Beattie and Poling studied arsenopyrite oxidation using cyclic voltammetry and X-ray photoelectron spectroscopy. They concluded that the oxidation of arsenopyrite results in the formation of ferric hydroxide surface layers above pH = 7. According to the same study arsenic is oxidized to arsenate and sulphur to sulphate, which diffuses into the solution while arsenate is adsorbed on the electrode surface. Buckley and Walker (1988/1989) noted that arsenopyrite oxidizes rapidly in air. They also reported that FeAsS is quickly oxidized in basic and acidic media and that As (-I) is more affected than Fe (II), while S (-I) is almost unaffected. Richardson and Vaughan (1989) have undertaken a spectroscopic study about arsenopyrite oxidized by a range of inorganic oxidants. The altered surface was investigated using various spectroscopic techniques and the conclusions obtained were discussed in relation to arsenopyrite extraction by flotation and leaching. The breakdown of arsenopyrite in natural systems and through the application of a potential was considered as well. The results indicated that the sulphur concentration in the surface layer could be influenced by the chemical conditions. Arsenic soluble compounds were referred to as prevalent in the altered surfaces and ferrous and ferric arsenites and arsenates formation was reported. Sanchez and Hiskey (1991) conducted a mechanism about the electrochemical behaviour of arsenopyrite in basic media in the presence and in the absence of cyanide. In agreement with these authors a two-step reaction sequence was suggested by electrochemical measurements. The initial step results in the formation of $Fe(OH)_3$, S^0

and $H_2AsO_3^-$, and the second one involves a combination of the oxidation of sulphur to sulphate and of the arsenite species to arsenate. Duc (1992) has documented the effects of grinding (dry or wet) and washing with different solutions and noticed that oxidized arsenic compounds were formed by the contact of the powders with aqueous solutions. The surface oxidation of arsenopyrite in alkaline solutions was also investigated by Wang et al. (1992) using cyclic voltammetry concerning mineral flotation. Ferric hydroxide and a realgar-like compound (AsS) were reported as produced in the initial stages of oxidation and both are retained on the arsenopyrite substrate. At higher potentials, the formation of sulphur and arsenate was mentioned. Nesbitt et al. (1995) showed that arsenopyrite oxidation in air and water leads to the formation of iron (III) hydroxi-oxide, arsenates and arsenites detected on the mineral surface. They are in agreement with other authors about the oxidation ability of the different elements with As being the more reactive. In addition, they also conclude that, as in the case of pyrite, the composition of the oxidized surfaces is strongly dependent on the experimental conditions. Finally, Nesbitt and Muir (1998) extend their research, reporting on the oxidation of the sulphide mineral by mine waste waters, drawing essentially the same conclusions.

In the present paper and together with electrochemical studies, X-ray photoelectron spectroscopy and Raman spectroscopy were used to identify the products of arsenopyrite oxidation formed during anodic treatment in acidic chloride solutions (+0.8 V (SCE) applied potential for 1 h). Previous research with a refractory arsenopyrite concentrate (Abrantes and Costa, 1996) showed that a similar electrochemical treatment allow the subsequent recovery of the occluded gold. Therefore, the data obtained are used to understand the mechanism of arsenopyrite transformation, leading to the release of the precious metals occluded in the sulphide matrix.

2. Experimental

2.1. Materials

In this study a concentrate and three natural mineral samples of high purity were used: arsenopyrite (AsFeS) and pyrite (FeS_2), which respectively came from Minas da Panasqueira and Aljustrel, both located in Portugal and galena (PbS) originating from the Iberian Pyrite Belt. A Portuguese arsenopyrite concentrate—chemical and estimated mineral composition described in Tables 1 and 2—from Jales Mine was also used.

Careful examination along a polished section with X-ray diffraction and optical microscopy showed the mineral samples to be of high purity. Their purity was also confirmed by chemical analysis of the trace elements. A standard polished thin section of the arsenopyrite crystal was prepared and analysed by an electron microprobe (Jeol Superprobe model 733). The average of 14 analyses at different points revealed the following stoichiometry: Fe = 33.83%, As = 46.80%, S = 18.39%, which is in agreement with a S-deficient and As-enriched specimen.

For the electrochemical experiments arsenopyrite, pyrite and galena electrodes were prepared by cutting rectangular prisms from the natural massive specimens. A compact

Table 1
Chemical composition of the arsenopyrite concentrate

Element/gangue	Content	
	%	mg/kg
Fe	28.46	
As	14.03	
S	30.40	
Pb	7.57	
Zn	2.76	
Cu	0.28	
Ag		420
Au		208
SiO_2	4.24	
CaO	2.37	
Al_2O_3	0.41	

disk electrode was also prepared from the concentrate (size range from 15 to 125 μm) using graphite powder ($\phi \sim 100$ μm) as a binder (20%). The mixture was cold pressed at 1.475×10^3 MPa for 15 min. Compact concentrate disk and mineral slabs were sealed with epoxy resin into "Teflon" holders.

For XPS analysis a cylindrical-shaped crystal (~ 1 cm diameter) of the arsenopyrite mineral was used.

Only samples free from visible inclusions, cracks and voids were used.

The exposed surfaces of the minerals and the concentrate were ground flat on 600 grit silicon carbide paper and hand-polished with an aqueous suspension of alumina (decreasing grain size down to 0.05 μm) and rinsed in distilled water.

2.2. Electrochemical experiments

The mineral electrodes were installed in a conventional three-electrode glass cell where a platinum foil was used as a counter electrode and a saturated calomel electrode (SCE) as the reference. The electrolyte solution (1.9 M NaCl + 0.1 M HCl) with a pH = 1.5, was prepared from analytical grade reagents with distilled water. Electro-

Table 2
Mineral composition of the arsenopyrite concentrate

Mineral	Weight (%)
Arsenopyrite	30.41
Pyrite	40.28
Galena	8.74
Sphalerite	4.11
Chalcopyrite	0.81

chemical characterization of the concentrate and pure minerals (arsenopyrite, pyrite and galena) and electrochemical treatment — electro-oxidation — of the arsenopyrite mineral were performed, at room temperature, with an EG&G PAR model 273A Potentiostat/Galvanostat programmed by a Triudus PC (electrochemical analysis model 270 software). The electrochemical behaviour has been analysed by cyclic voltammetry, starting from near the open circuit potential, with 50 mV/s potential scan rate. The potential domain was extended from oxygen to hydrogen evolution regions.

Electro-oxidation of the arsenopyrite concentrate — previously described in the literature (Abrantes and Costa, 1996; Costa, 1996) — was carried out in chloride media (NaCl 1.9 M + HCl 0.1 M) for 2 h at room temperature. A current density of 44 A/m^2 was used to guarantee an anodic potential of +0.8 V. A particulated bed anode of the concentrate — 10% slurry density — was utilised in a two-compartment cell with a graphite rod anode feeder and a stainless steel cathode. A magnetic bar was employed to stir the solid particles in the anodic compartment. The electro-oxidized residue was finally leached with an acidic thiourea solution under the experimental conditions previously reported (Abrantes and Costa, 1996; Costa, 1996).

In order to produce similar alterations to the surface as those produced during electro-oxidation of the arsenopyrite concentrate (Abrantes and Costa, 1996; Costa, 1996), the arsenopyrite electrode potential was stepped positively to 0.8 V for 1 h.

2.3. Surface analysis

2.3.1. X-ray photoelectron spectroscopy

X-ray photoelectron spectra were recorded using a XSAM 800 (KRATOS) X-ray spectrometer operated in the fixed analyser transmission (FAT) mode with a pass energy of 10 eV and the non-monochromatic Mg-K_α X-radiation ($h\nu = 1253.7$ eV). Typical operating parameters were 13 kV and 10 mA. Samples were analysed in ultra high vacuum (UHV), and typical base pressure in the sample chamber was in the range of 10^{-7} Pa. All sample transfers were made in air. Samples were analysed at room temperature, at analysis angles of 0° and 60° relative to the normal to the surface. Spectra were collected and stored in 200 channels with step of 0.1 eV, and 60 s of acquisition by sweep, using a PDP-11/73 microcomputer from Scientific Micro Systems using DS800 software, from Kratos, for spectral acquisition, storage and processing. The curve fitting was carried out with a non-linear least-squares algorithm using a mixed Gaussian–Lorentzian peak shape. A Shirley background was subtracted to all fitted spectra. For energy calibration purposes, in order to correct charging effects, the C 1s peak from the aliphatic contaminants was considered to be at a binding energy of 285 eV (Beamson and Briggs, 1992).

2.3.2. Raman spectroscopy

Raman spectra were recorded on a SPEX 1403 spectrometer consisted on a double spectrograph. The grating was 1200 groves/mm and the final slit width 160 μm. Monochromatic light with a wavelength of 514.5 nm from an argon-ion laser (Spectra Physics, model 164-05) was used as exciting source with an incident power of 220 mW at the sample.

2.4. Solution analysis

A Dionex 4000I ion chromatograph (model DX 300) with conductivity detection was utilised to analyse the solution after electrolysis. Sulphite and sulphate were determined with a Dionex AS4A column and a 1.8 mM Na_2CO_3 + 1.7 mM $NaHCO_3$ solution was used as eluent at 2 cm^3/min.

Atomic Absorption Spectroscopy (AAS) (Pye Unicam SP9 Model coupled with a Philips Model 910 Computer) was used to analyse the solutions resulting from the chemical attack of the materials and the pregnant electroleaching solution. Gold and arsenic was analysed by inductively coupled plasma (ICP) spectroscopy (ARL-Fison 3410).

3. Results and discussion

3.1. Electrochemical characterization

The possibility of using an electrochemical process as a pre-treatment for the recovery of gold from refractory complex sulphide concentrates has been revealed by the voltammetric response given by an electrode prepared from the raw material. As shown in Fig. 1, during cyclic voltammetry of the arsenopyrite concentrate electrode (carbon paste electrode), in chloride medium, starting from the open circuit potential and scanning the potential anodically, several oxidation/reduction reactions can be observed, which give rise to the formation of solid and soluble products. Different mineral

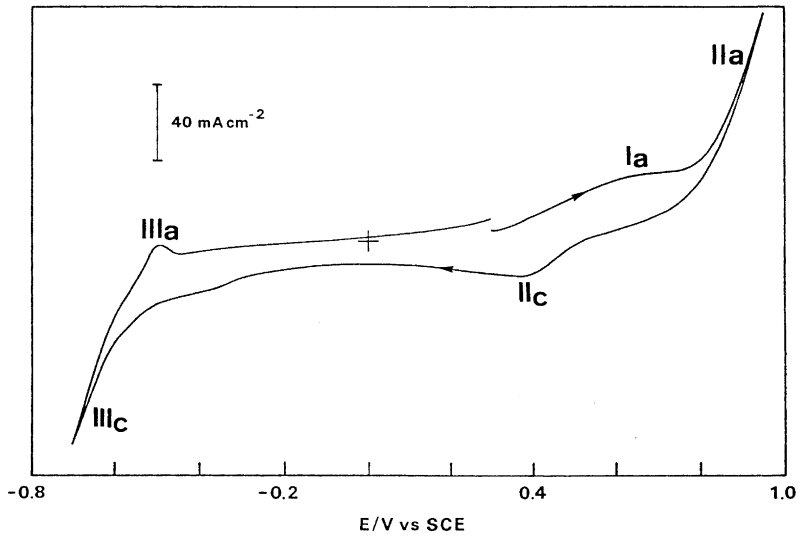

Fig. 1. Cyclic voltammogram of arsenopyrite concentrate electrode (carbon paste electrode) in 1.9 M NaCl + 0.1 M HCl; $v = 50$ mV/s.

species — arsenopyrite, pyrite and galena — present in the arsenopyrite concentrate (see its mineralogical composition on Table 2) contribute to the overall behaviour.

This can be easily seen by contrasting the cyclic voltammogram of Fig. 1 to the results obtained under similar conditions for arsenopyrite, pyrite and galena minerals (Fig. 2).

The anodic peak that is seen in the voltammogram of the concentrate at about +0.55 V (vs. SCE) — peak Ia — being due to the dissolution of the three main mineral constituents, receives a special contribution from galena, which reacts forming Pb^{2+} and S^0 at low potentials (Pritzker and Yoon, 1988). The dissolution of the iron sulphides occurs with the formation of intermediate compounds such as $Fe_{1-x}As_{1-y}S$ and $Fe_{1-x}S$ (Sanchez and Hiskey, 1991; Ahlberg et al., 1990).

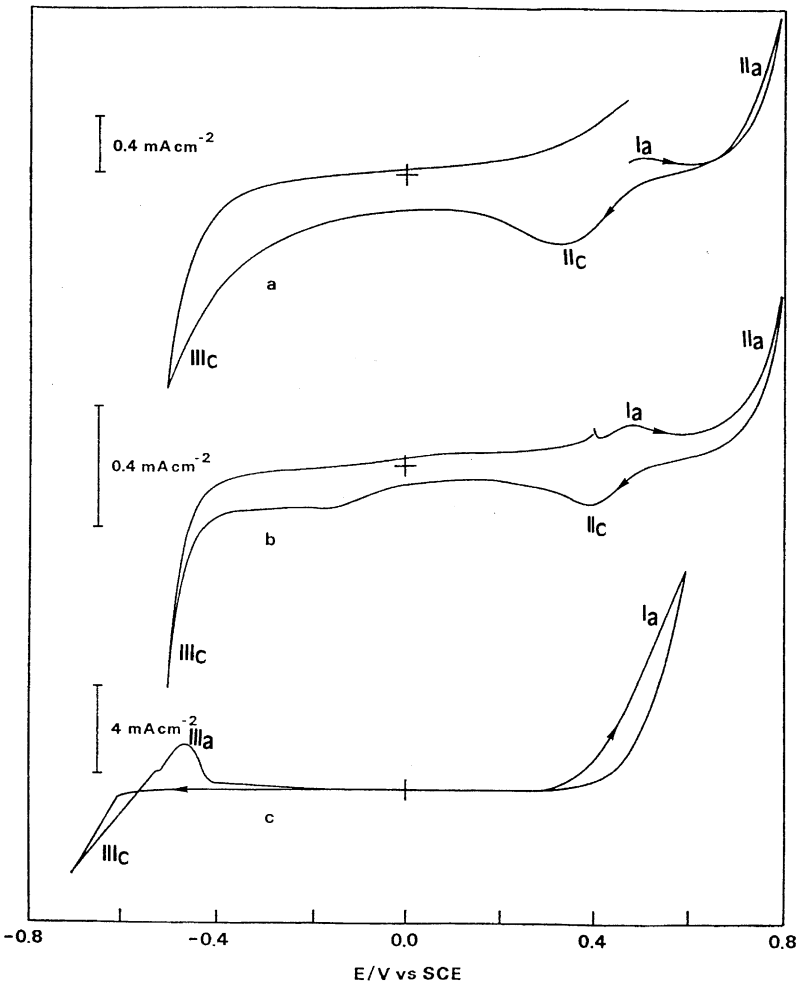

Fig. 2. Cyclic voltammograms for arsenopyrite (a), pyrite (b) and galena (c) electrodes in 1.9 M NaCl + 0.1 M HCl; $v = 50$ mV/s.

The anodic wave denoted by Ia in the voltammogram of arsenopyrite — Fig. 2 — is associated with several oxidation reactions, giving rise to intermediate sulphides (e.g. As_2S_2 and As_2S_3), which are quickly oxidized to S^0 (Beattie and Poling, 1987); the formation of arsenic oxides shall also be considered. Close to the anodic limit the voltammetric response of the concentrate presents a sharp current increase (IIa) and this feature is also observed for pyrite and arsenopyrite. This behaviour is likely to be associated with the oxidation of the hitherto formed sulphur to oxy-sulphur species such as $S_xO_y^{2-}$ and S_x^{2-} (Costa, 1996; Wiand, 1991). On the return (negative direction) scan, these products are reduced yielding a cathodic peak (IIc) at about +0.4 V (SCE).

The current increase denoted by IIIc (Figs. 1 and 2) is due to the reduction of S^0 to H_2S. The recombination of Pb^{2+} and S^0 previously formed leading to the formation of PbS also contributes towards the current increase verified in Fig. 2c. In addition, metallic lead can deposit on the PbS surface when the potential decreases below about −0.55 V (SCE).

Reversing the scan direction, the anodic peak — IIIa — present in the voltammogram of the concentrate at about −0.5 V (SCE) is due to the presence of galena, as it can be seen by the current response of the PbS electrode. For galena, two distinct peaks are clearly observed. One is probably related to the oxidation of lead and formation of chloro-complexes and the other can be associated with the oxidation of the H_2S previously formed.

In order to investigate the surface transformations produced by electro-oxidation, the arsenopyrite mineral has been submitted to controlled potential electrolysis under the same conditions, which allows the subsequent recovery of gold when the procedure is applied to the gold containing arsenopyrite concentrate. Based on the experimental evidence obtained in the electrochemical study, four anodic potential values were chosen and the current evolution is displayed in Fig. 3.

For potentials higher than +0.6 V there is a current increase during the first minutes but thereafter the signal is dependent on the applied potential, although a decrease is always observed after a given time. The current decrease is consistent with the growth of a layer of elemental sulphur, which tends to render the electrode passive.

However, in addition to the sulphur, other surface products must be taken into account. Other methods than the electrochemical need to be considered to characterize the yellowish layer produced on the mineral surface when subjected to +0.8 V (SCE) for 1 h in chloride solution. It should be emphasised that an anodic potential of +0.8 V (SCE) was selected for the electro-oxidation process considering the electrochemical behaviour of the concentrate and arsenopyrite mineral. Near this value the voltammograms of the concentrate and pure mineral show a high oxidative current able to modify the sulphide matrix in which the gold is usually included or occluded and therefore render the precious metal amenable for subsequent recovery.

3.2. X-ray photoelectron spectroscopy

In this study XPS peak area intensity ratios were used to measure the stoichiometry of the sulphide surface before and after electrochemical treatment — +0.8 V for 1 h in NaCl 1.9 M + HCl 0.1 M solution — as a function of depth into the surface. Two

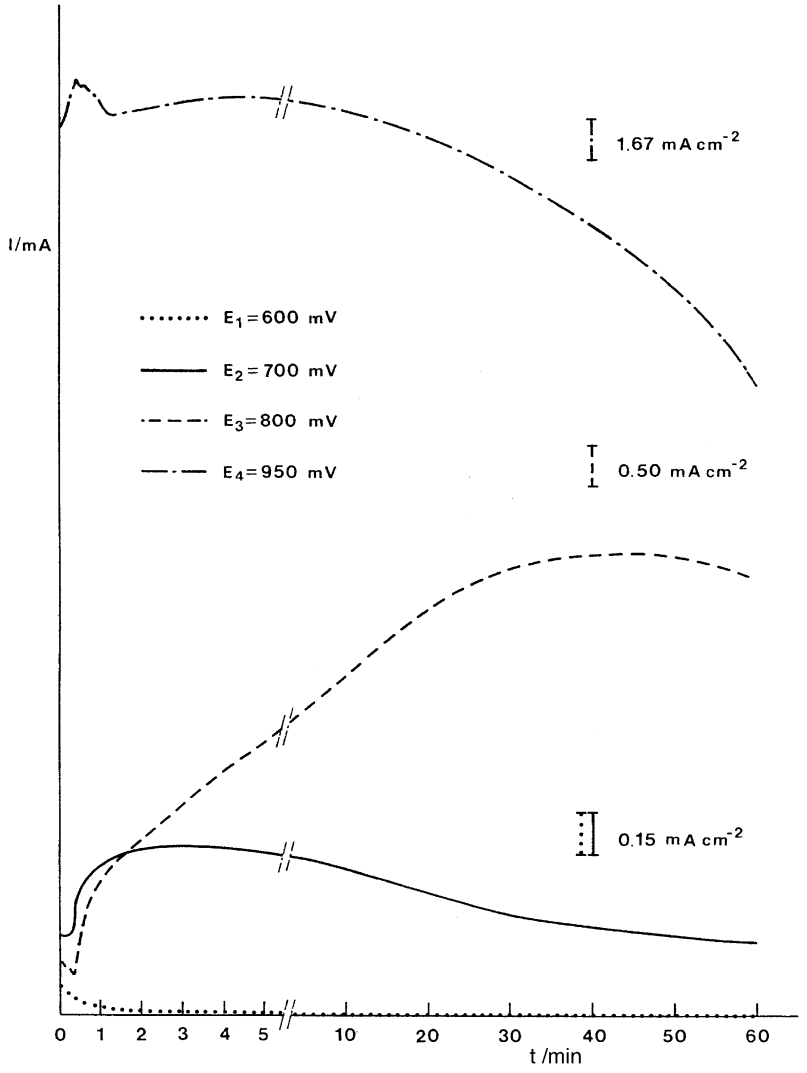

Fig. 3. Current density evolution over time for arsenopyrite mineral in 1.9 M NaCl + 0.1 M HCl.

different analysis angles — 0° and 60° relative to the normal to the surface — were used in order to check for the possible existence of elemental concentration gradients in depth. It should be pointed out that the surface before electrochemical treatment was exposed to air after its polishing and before its placement in the vacuum chamber.

Fig. 4 shows S 2p, As 3d and Fe 2p spectra — a, b and c, respectively — of the arsenopyrite mineral before electrochemical treatment for the two angles used.

The global quantification of the mineral surface using the total areas in Fig. 4 for each element after a Shirley background subtraction, yield the following stoichiometry: Fe = 24.58%, As = 33.05%, S = 42.37% and Fe = 25.10%, As = 34.41%, S = 40.48% for

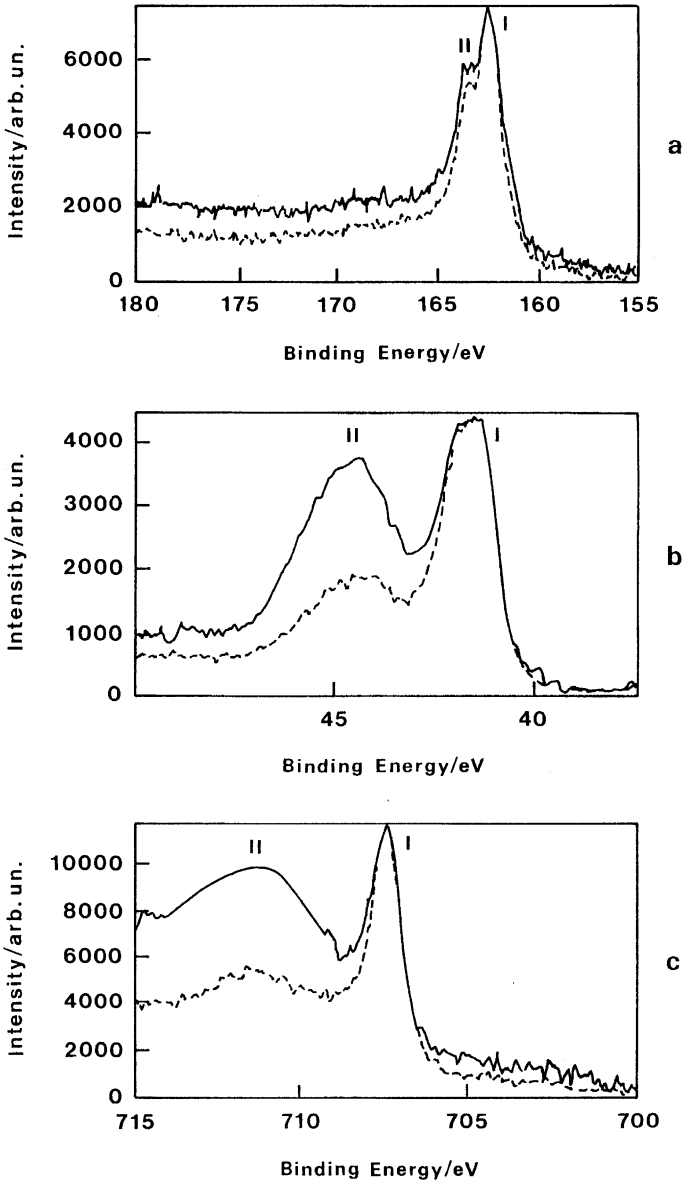

Fig. 4. Normalized X-ray photoelectron spectra of arsenopyrite, before electrochemical treatment, as a function of depth analysis; two angular studies: $\theta = 0°$ (- - - -) and $\theta = 60°$ (——); (a) S 2p; (b) As 3d; (c) Fe 2p.

the analysis carried out at $\theta = 0°$ and $\theta = 60°$, respectively. In contrast to the bulk, this stoichiometry is typical of a metal deficient and rich in sulphur surface. The difference between the bulk and the surface composition can indicate sulphur segregation due to an arsenic and iron deficiency caused by the oxidation of these elements. Taking into

account the most common binding energies for Fe $2p_{3/2}$, As $3d_{5/2}$ and S $2p_{3/2}$ in arsenopyrite and other sulphide minerals summarised in Table 3, and also the doublet splitting contained in Table 4, we can assign peak II to the oxidized species. The exception is S 2p where the peak I corresponds to the S $2p_{3/2}$ component and the peak II to the S $2p_{1/2}$ component.

Therefore, according to these spectra, the arsenopyrite surface is already oxidized even before any treatment due to its exposure to air. These results are in accordance with the work of Richardson and Vaughan (1989), who refer that the oxidation of arsenopyrite occurs spontaneously in the presence of air. However, as mentioned by the same authors, arsenopyrite is slowly oxidized and oxidants are generally required to accelerate oxidation. The ratio A_{II}/A_I, where A_I and A_{II} are the areas of peaks I and II, respectively, increases from $\theta = 0–60°$, for the Fe 2p and As 3d peaks, which is in accordance with a more drastic oxidation near the surface due to contact with air. The increasing of the ratio cited above means that the outer surface is richer in oxidized species than the bulk.

Assuming a schematic model with an oxide layer, homogeneous in depth, covering the non-oxidized material, a more quantitative analysis can be done. In fact, in that situation, the ratio A_{II}/A_I for a given species, X, should be approximately (Briggs and Rivière, 1996):

$$A_{II}/A_I(X) \alpha e^{\rho/\lambda X \cos\theta} - 1$$

where ρ is the thickness of the oxide layer and λ_X is the effective attenuation length. On the other hand, the ratio $r_X = A_{II}/A_I(X)_{\theta=60°}/A_{II}/A_I(X)_{\theta=0°}$ depends only on the ratio

Table 3
XPS binding energies (eV) for Fe $2p_{3/2}$, As $3d_{5/2}$ and S 2p in several chemical environments

	Chalcopyrite	Pyrite	Loellingite	Arsenopyrite	FeO	Fe_2O_3	$FeSO_4$	$Fe_2(SO_4)_3$
Fe $2p_{3/2}$	706.9[a]	707.0[a,b,c,d] 707.1[j,k] 707.4[j] 707.5[n] 707.9[o]	707.0[e]	706.9[f] 707.0[e] 707.1[j] 707.2[c]	709.5[g] 709.6[l]	710.9[h,*] 711.0[a,f,g,j,m] 711.6[l]	711.3[i,**] 712.3[f]	713.5[i] 714.6[f]
	Arsenopyrite	As_2S_3	As_4S_4	As_2S_5	As_2O_3	As_2O_5		
As $3d_{5/2}$	41.0[p] 41.2[e,t] 42.1[j]	43.4[q] 43.6[r] 43.8[j]	43.2[j] 43.4[q]	44.4[r]	43.9[s] 44.5[e,q,u] 44.7[j,w] 44.9[v] 45.4[h,x]	45.3[q,e] 45.9[v] 46.3[x] 46.5[y]		
	Chalcopyrite	Pyrite	Arsenopyrite	S^0	$S_2O_3^{2-}$	SO_3^{2-}	SO_4^{2-}	
S $2p_{3/2}$	160.8[a] 161.1[bb] 161.2[f]	162.1[a] 162.3[j] 162.4[dd] 162.5[f]	162.4[c] 162.7[j]	163.5[a] 163.6[bb] 164.0[b,ee]	167.0[z]	166.2[aa] 166.8[cc] 167.7[ee]	168.3[a] 168.4[j] 168.5[bb]	
S $2p_{1/2}$	163.2[a]	161.9[a] 162.3[bb]	163.6[c]					

Table 4
Doublet splitting for Fe 2p, As 3d and S 2p

Photoelectron	Doublet splitting (eV)
Fe 2p	~ 13
As 3d	0.7–1
S 2p	1.05–1.2

ρ/λ_X, which can be calculated for each element. Assuming that both Fe and As are oxidized over the same depth, we can finally obtain ρ. Assuming also that $\lambda_{As} \sim 14$ Å and $\lambda_{Fe} \sim 25$ Å, typical values of inelastic mean free paths in inorganic compounds (Tanuma et al., 1991), we obtain $\rho = 16.4$ Å from $r_{Fe}(=3.2)$ and $\rho = 21.9$ Å from $r_{As}(=2.41)$. Given the large errors that can be made in the area calculation, especially in the case of Fe, due to the background subtraction and to the extreme assumption

Notes to Table 3:
[a] (Buckley and Woods, 1984).
[b] (Mycroft et al., 1990).
[c] (Pratt et al., 1998).
[d] (Nesbitt and Muir, 1994).
[e] (Nesbitt et al., 1995).
[f] (Richardson and Vaughan, 1989).
[g] (McIntyre and Zetaruk, 1977).
[h] (Mielczarski et al., 1996b).
[i] (Brion, 1980).
[j] (Hacquard et al., 1999).
[k] (Egglestbon et al., 1996).
[l] (Mills and Sullivan, 1983).
[m] (Harvey and Linton, 1981).
[n] (Chaturvedi et al., 1996).
[o] (Pillai and Bockris, 1985).
[p] (Duc, 1992).
[q] (Fullston et al., 1999).
[r] (Wagner et al., 1979).
[s] (Grunthaner et al., 1979).
[t] (Buckley and Walker, 1988/1989).
[u] (Mielczarski et al., 1996a).
[v] (Mizokawa et al., 1978).
[w] (Breeze et al., 1980).
[x] (Bertrand, 1981).
[y] (Stec et al., 1972).
[z] (Knipe and Fleet, 1997).
[aa] (Fornasiero et al., 1994).
[bb] (McCarron et al., 1990).
[cc] (Fairthorne et al., 1997).
[dd] (Scaini et al., 1997).
[ee] (Moulder et al., 1992).
* This value is recorded for iron hydroxi-oxide.
** This value is recorded for $FeSO_4 \cdot 7H_2O$.

about the oxidized overlayer homogeneity, we can consider these two values compatible. In fact an error of 10% in each area, can lead to errors larger than 40% in the ratios r_X from which we obtain the layer thickness. Thus, we can say, that the oxide layer has a thickness in the order of 2 nm. This value is in agreement with the value obtained by Hacquard et al. (1999) (2–3 nm) for a crude estimation of the thickness of an oxidation layer formed after the arsenopyrite comes into contact with an aqueous solution at pH = 10.

The XPS results obtained for the electro-oxidized surface indicated the following global stoichiometry: Fe = 5.00%, As = 11.67%, S = 83.33% for $\theta = 0°$ and Fe = 12.92%, As = 19.05%, S = 68.03% for $\theta = 60°$. It can be inferred from these results that the surface layer observed after electrochemical treatment — a grey yellowish layer was obtained on the mineral surface by the application of the anodic potential — is due to the formation of elemental sulphur, which is reported to be formed in acidic conditions (Pritzker and Yoon, 1988; Beattie and Poling, 1987; Zheng and Lin, 1994). The decrease in the amounts of As and Fe relative to sulphur and the higher proportion of Fe and As for the analysis performed at $\theta = 60°$, is in agreement with the oxidation mechanism proposed by Peters (1984). In fact, he considers that the oxidation process of the components of mineral sulphides occurs by preferential removal of iron to probably form a layer of iron oxide. In alkaline solutions iron precipitates on the surface as hydroxide, leaving a reacted layer of elemental sulphur. Buckley and Woods (1984) carrying out studies by electrochemical and surface spectroscopy techniques showed that the initial oxidation of sulphide minerals in general proceeds through a progressive removal of metal atoms, which leaves the sulphur lattice largely unaltered. Other research also attested to the formation of sulphide-rich surfaces in the initial oxidation phase (Turcotte et al., 1993; Li et al., 1993; Mycroft et al., 1990).

The results of XPS analysis of arsenopyrite surface before and after electrochemical treatment are shown in Figs. 5–7.

After electro-oxidation the surface of AsFeS is obviously deeply oxidized. The presence of phases with higher binding energies than arsenopyrite is observed in all figures, even before electrochemical treatment. This is interpreted as various oxidized phases resulting from the exposure of the mineral surface to air after its fracture and polishing and before its placement in the vacuum chamber. Table 5 shows the XPS binding energies assigned to the arsenopyrite components.

Table 5
XPS binding energies (eV) assigned to arsenopyrite components (this work)

	Arsenopyrite	FeO	Fe_2O_3	S^0	SO_4^{2-}	As_2O_3	As_2O_5
Fe $2p_{3/2}$	707.3	709.6	711.4a* 711.8b*	–	–	–	–
As $3d_{5/2}$	41.5	–	–	–	–	43.9	45.4
S $2p_{3/2}$	162.4	–	–	164.0	168.0a* 168.8b*	–	–

* Different BE values, were obtained in the spectra of arsenopyrite before (a) and after electro-oxidation (b).

3.2.1. S 2p spectra

The spectra of Fig. 5 are the S 2p spectra of arsenopyrite before (a) and after (b) electro-oxidation obtained with an analysis angle of 0°. In this case no considerable differences were observed for the analysis performed at 60°. The S 2p spectra were fitted with doublets consisting of two peaks (3/2 and 1/2) resulting from spin–orbit splitting, separated by 1.1–1.2 eV, with the intensity of the lower binding energy peak being double that of the higher binding energy peak. The S 2p spectrum of the mineral exposed to air (Fig. 5a) was fitted with four doublets. The first one (I) is clearly

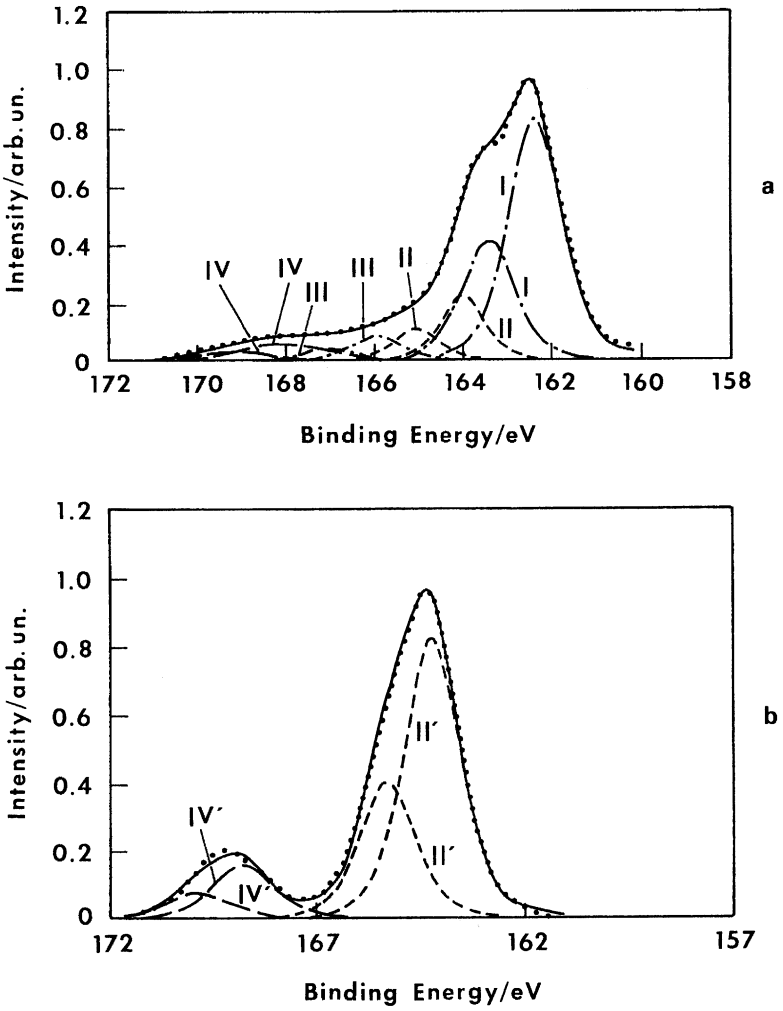

Fig. 5. X-ray photoelectron S 2p spectrum for arsenopyrite: (a) before electro-oxidation; (b) after electro-oxidation. The dots represent the experimental sprectrum, and the full line represents the calculated spectrum obtained by summing all of the mixed Gaussian–Lorentzian bands.

predominant and can be assigned to the arsenopyrite mineral since the BE of the S $2p_{3/2}$ main peak is 162.4 eV. This is in full agreement with binding energies reported in the literature for arsenopyrite (see for example Pratt et al., 1998, and other references cited therein). This BE value is similar to typical BE for pyrite (in both sulphide minerals sulphur is in -I oxidation state), which has typically a BE 1.3 eV greater than chalcopyrite (where sulphur is in -II oxidation state) — see Table 3. In fact, peaks resulting from S bonded to As (S–As) and S bonded to S (S–S) are reported as having essentially the same BE (Nesbitt et al., 1995), which contributes to no S (2p) distinct peaks for arsenopyrite and pyrite. The other three doublets are due to arsenopyrite oxidation products, and various oxidation states from S(0) to S(VI) can be identified in this spectra. The second doublet — (II) S $2p_{3/2}$, 164.0 eV — is assigned to elemental sulphur (Moulder et al., 1992; Mycroft et al., 1990), which seems to be the most important oxidation product. Taking into account the long tail of the spectrum at binding energies between 165 and 170 eV, two more doublets (III and IV) can be fitted and attributed to higher sulphur oxidation states. The values for the BE of S $2p_{3/2}$ for the third and fourth doublets, 166.0 and 168.0 eV, respectively, are consistent with the presence of oxy-sulphur species in +2 and +6 oxidation states and, therefore, the formation of some tiosulphate ($\sim 167 \pm 1$ eV) and sulphate ($\sim 169 \pm 1$ eV) should also be considered (Rinker et al., 1997). In the S 2p spectrum of the mineral after electrochemical oxidation (Fig. 5b), no peaks were observed at the binding energies expected for the mineral sulphide. Hence, the arsenopyrite surface was completely transformed mainly to elemental sulphur, to which doublet II′ is assigned (S $2p_{3/2}$— 164.2 eV). This result is in agreement with the observation of a yellowish layer in the electrode surface after the application of the anodic potential. A second doublet (IV′) with a S $2p_{3/2}$ binding energy of 168.8 eV characteristic of the presence of sulphate, was also fitted, this compound being identified in both spectra. A different combination of various oxy-sulphur compounds on the surface can also be responsible for some differences in that region of both spectra. It should be noted that the oxidation of sulphur to oxy-sulphur species has already been mentioned in the cyclic voltammetry interpretation as occurring at the anodic potential used. The formation of sulphite and sulphate species as a result of the arsenopyrite electro-oxidation was also detected in the solution of the electrochemical treatment by ionic chromatography, confirming the XPS results. The presence of polysulphide species already referred to by other authors (Mycroft et al., 1990) as intermediate oxidation products of several sulphide minerals was not detected since no peaks with intermediate BE between arsenopyrite and elemental sulphur were found (a BE value of 163.3 eV was interpreted by Nesbitt et al. (1995), as belonging to polysulphides S_x^{2-}).

3.2.2. As 3d spectra

The spectra of Fig. 6 are the As 3d spectra of arsenopyrite before (a) and after (b) electro-oxidation with an analysis angle of 0°. Each spectrum is composed of (5/2, 3/2) doublets consisting of two peaks separated by 0.8–1 eV, with the intensity of the higher binding energy peak being two-thirds that of the lower binding energy peak. For spectrum 6a, three 5/2, 3/2 doublets were fitted. The first one (I) is the most intense and has a $3d_{5/2}$ BE of 41.5 eV that can be assigned to the sulphide mineral. The

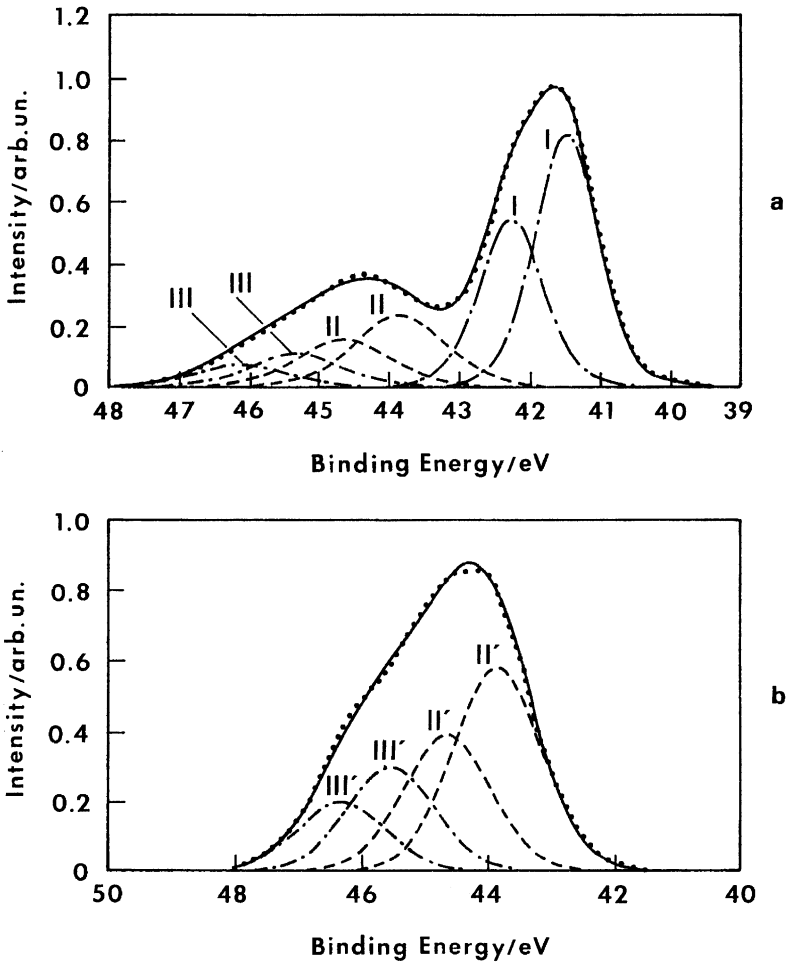

Fig. 6. X-ray photoelectron As 3d spectrum for arsenopyrite: (a) before electro-oxidation; (b) after electro-oxidation. The dots represent the experimental sprectrum, and the full line represents the calculated spectrum obtained by summing all of the mixed Gaussian–Lorentzian bands.

presence of phases with higher binding energies (doublets (II) and (III)) is interpreted as various oxidized phases, the values of As $3d_{5/2}$ — 43.8 eV and 45.3 eV — being consistent with a range of arsenic (+3) and arsenic (+5) compounds, respectively. The binding energies of the As 3d peaks reported in this study are similar to those obtained in earlier XPS studies. Thus, according to the literature the second value can be clearly attributed to arsenate, As_2O_5, while the first one can be associated with either arsenite, As_2O_3, or arsenic sulphides. Arsenic sulphides have already been mentioned as probable oxidation products in the electrochemistry section. Although the formation of arsenic sulphide species has been mentioned in previous studies (Abrantes and Costa, 1996; Beattie and Poling, 1987) as intermediate oxidation products, their identification

is difficult because their binding energies are very close to those of the arsenic oxides (see values of Table 3). Peaks for As_4S_4, As_2S_3 and As_2S_5 are reported at 43.1, 43.4 and 44.4 eV, respectively, at BE approximately 1 eV lower than their corresponding arsenic oxides (Wagner et al., 1979). In the As 3d spectrum of the mineral after electro-oxidation (Fig. 6b) no peaks were found at the binding energies expected for the mineral sulphide. This is in accordance with the results already obtained for sulphur, confirming the complete transformation of the mineral surface. The As $3d_{5/2}$ peaks observed in this case at 43.9 eV (II′ doublet) and 45.5 eV (III′ doublet), are consistent with the same arsenic oxidation products previously mentioned (arsenic (III) and arsenic (V) oxides and eventually arsenic sulphide species). Therefore, in the electro-oxidized surface arsenic (III) and (V) are the major compounds, which indicates that the rate of formation of the oxidized phases is greater than their dissolution from the surface (Richardson and Vaughan, 1989), although the high solubility reported for arsenic (III) oxides (~ 20 g/l, Wedepohl, 1978) and even much higher for arsenic (V) oxides (65.8 g/100 ml at 20 °C, Perry's Chemical Handbook, 1984; Nesbitt et al., 1995) suggest that the composition of the oxidation layer might be properly described by a mixture of ferric arsenate and ferric arsenite.

The electro-oxidized arsenopyrite spectrum obtained with an analysis angle of 60° (more superficial analysis) is similar to spectrum Fig. 6b, although the peaks that correspond to doublet III′ show in this case the highest intensities. This indicates the predominance of As_2O_5 over As_2O_3 near the outer surface and therefore a more drastic oxidation close to the surface, supporting the idea of concentration arsenic compounds gradients.

3.2.3. Fe $2p_{3/2}$ spectra

Fe $2p_{3/2}$ spectra for arsenopyrite before and after electrochemical treatment, obtained with an analysis angle of 0°, are found in Fig. 7a and b, respectively. No considerable differences were found for the analysis carried out at 60°. Although some authors have used both chemical shift and multiplet splitting effects of the Fe 2p line (calculated from theory by Gupta and Sen, 1974, taking into account spin–spin and spin–orbit interactions) for fitting procedures, a simplified peak fitting approach was used in this study. Rather than including many fitting parameters (even if they can be physically justified), we simply fitted the Fe $2p_{3/2}$ spectra using a minimum number of peaks. Hence, the Fe $2p_{3/2}$ spectrum of Fig. 7a can be resolved into four peaks (I to IV): a very intense and narrow at 707.3 eV (peak I) and three weaker and broader at 708.8 (peak II), 711.4 (peak III) and 714.3 eV (peak IV), constituting a tail-off of intensity toward higher BE. The Fe $2p_{3/2}$ peak at 707.3 eV is assigned to FeAsS in agreement with the literature (Hacquard et al., 1999; Pratt et al., 1998). Results obtained from loellingite ($FeAs_2$) and pyrite (FeS_2) showed that Fe(II) bonded to As–As or to S–S has essentially the same BE (Nesbitt et al., 1995). Thus, it can be admitted that Fe(II) bonded to As–S (as in arsenopyrite) falls within the same BE range, making it impossible to distinguish among arsenopyrite, Fe(II)–(As–S) bond, pyrite, Fe(II)–(S–S) bond and loellingite, Fe(II)–(As–As) bond (see values of Table 3). The tail-off of intensity in the 709–716 eV range is also common for pyrite, including for those samples fractured in ultra-high vacuum and has been partly attributed to inelastically

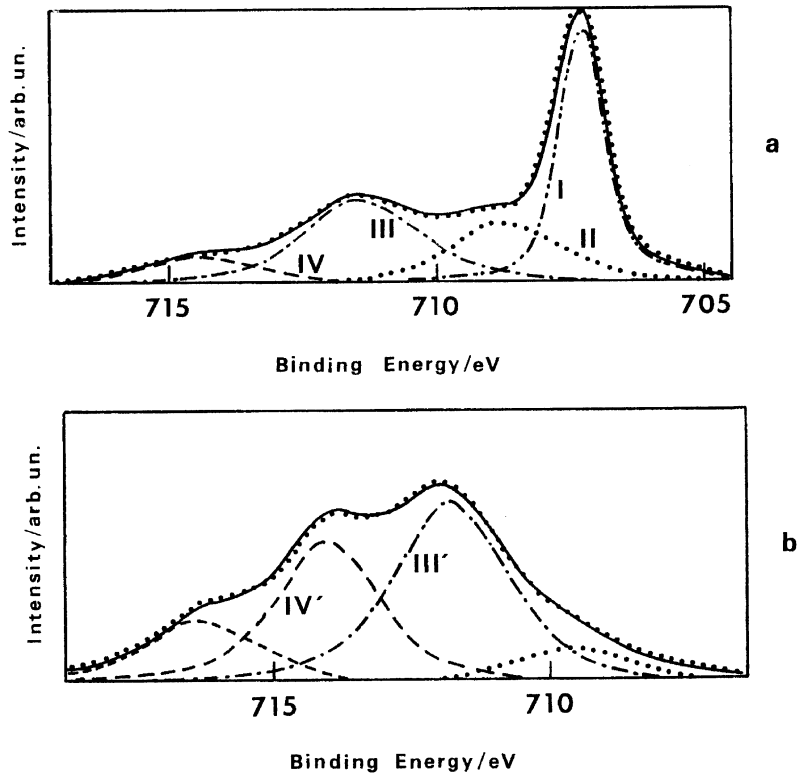

Fig. 7. X-ray photoelectron Fe $2p_{3/2}$ spectrum for arsenopyrite: (a) before electro-oxidation; (b) after electro-oxidation. The dots represent the experimental sprectrum, and the full line represents the calculated spectrum obtained by summing all of the mixed Gaussian–Lorentzian bands.

scattered electrons (Egglestbon et al., 1996). However, some authors (Karthe et al., 1993) argued that multiplet-splitting should not contribute to the intensity and other possible contributors for the tail-off Fe $2p_{3/2}$ peak have been considered. Therefore, and according to previous studies (Pratt et al., 1998; Rinker et al., 1997; Nesbitt and Muir, 1994; Karthe et al., 1993) the peak found at 708.8 eV may represent Fe bonded to S, which can be consistent with the fact that FeS has been reported as a possible oxidation product of pyrite (Pillai and Bockris, 1985; Frost et al., 1977). Furthermore, the possibility that FeS was a contaminant and therefore probably originally present in arsenopyrite crystal should not be ignored. Rinker et al. (1997) also refer to a major Fe $2p_{3/2}$ peak at 708.95 eV due to the Fe^{3+} −S bonds, which is consistent with the general acceptance that Fe(III)–S environments might contribute to the 709–712 eV region. The presence of Fe(III)−(As–S) bonds in the near surface of the mineral is another possible reason for the observed tail in this BE range (Nesbitt et al., 1995). Considering that Fe(III)–O environments resulting from oxidation occur at about 711–712 eV (Egglestbon et al., 1996), the Fe $2p_{3/2}$ peak observed at 711.4 eV can be assigned to

ferric oxides or oxy-hydroxides. Based on Egglestbon et al. (1996), some of these species can be defects that may be created by damaging of the arsenopyrite surface and which may disappear through oxidation. The peak observed at 714.3 eV is likely due to the presence of ferric sulphate. After electrochemical treatment spectrum Fig. 7b can be fitted equally using four peaks with the following BE: 709.6, 711.8, 714.1 and 716.2 eV. A significant increase in the peaks assigned to ferric oxides or oxy-hydroxides — 711.8 eV (peak III′) — and ferric sulphate — 714.1 eV (peak IV′) — as well as the complete transformation of arsenopyrite mineral, are observed in spectrum Fig. 7b. The peak at 709.6 eV can be due to the presence of ferrous oxide. However, Pratt et al., 1998 refer that in arsenopyrite, a peak at 709.8 eV may be associated with Fe–As groups at the outer surface, which can be consistent with the presence of ferric arsenate or arsenite, already mentioned. Iron (III) oxide seems to be the major iron phase in the electro-oxidized surface. The ratio between iron (II) oxide and iron (III) oxide components is closely related to the extension of oxidation. The highest BE peak at 716.2 eV is difficult to identify and its value is too low to be assigned to a Fe $2p_{1/2}$ component. It may be due to a multiplet structure.

XPS results obtained in the present investigation are in general in accordance with data from previous XPS studies. The results obtained show that the arsenopyrite surface is rapidly oxidized in the presence of air and is completely transformed by electro-oxidation. As expected, the electrochemical treatment produces a more drastic oxidation and at a higher rate than other oxidizing procedures previously reported (oxidation by air or by water — Nesbitt et al., 1995). Although essentially the same, oxidation products were detected in the arsenopyrite surface, electro-oxidation completely transforming the surface. Our results show that the rate of oxidation of Fe (II) and As (I) is more rapid than the rate of S (-I) oxidation in accordance with Buckley and Walker (1988/1989).

3.3. Raman spectroscopy

Raman spectroscopy was first recognised for identification and structural analysis of minerals by Griffith and White (1975). It is also often used to identify microscopic inclusions in the minerals, giving information that is difficult to obtain by other techniques such as electron microprobe and ion microprobe.

In this paper Raman spectroscopy was performed to confirm the formation of elemental sulphur on the mineral surface after anodic oxidation.

Fig. 8 shows the Raman spectra of arsenopyrite after 1 h electro-oxidation at +0.8 V (SCE); for comparison a literature spectra (Mernagh and Trudu, 1993) of non-electro-oxidized arsenopyrite (pristine arsenopyrite) is also shown. Although arsenopyrite produces a weak Raman spectra compared to other sulphide minerals, a total of six bands were observed, two of them with relatively high intensity (212 and 274 cm^{-1}). Most of these bands are quite broad, which could be due either to thermal effects or to the near coincidence of several Raman bands (Mernagh and Trudu, 1993).

After 1 h of anodic oxidation new features could be observed in the spectrum. The disappearance of all the typical bands of the pure mineral and the appearance of several intense and well-defined peaks must be pointed out. There is no difference between the Raman spectrum obtained and the typical ex-situ spectrum of elemental sulphur (Turcotte

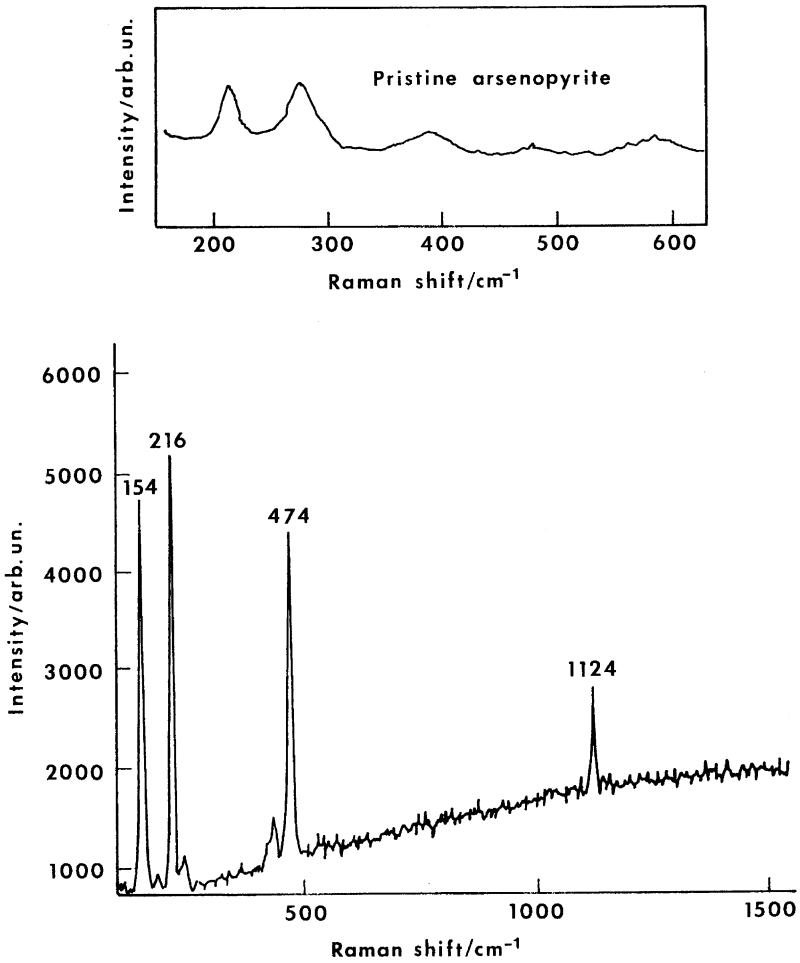

Fig. 8. Ex situ Raman spectrum of oxidation products on arsenopyrite surface, after 1 h of electro-oxidation at +0.8 V (SCE) in chloride solution (NaCl 1.9 M + HCl 0.1 M). The inset shows the Raman spectrum for pristine arsenopyrite.

et al., 1993). Thus, after 1 h of electrolysis under the tested conditions of potential (+0.8 V) and pH (pH = 1.5), sulphur clearly became the predominant surface component. Dunn and Fernandez (1987) had also observed the dissolution of arsenopyrite in KCl 0.1 M from pH = 2.4 to 11.8 and reported sulphur formation for potentials above +0.7 V. The peaks observed agree with previously published studies for oxidized pyrite and elemental sulphur (Vreugde, 1983; McIntyre and Zetaruk, 1977). An S–S stretching mode resulting in the Raman peak at 474 cm^{-1}, and S–S–S chain modes are responsible for the peaks at 154 and 216 cm^{-1}. The peak observed at 1124 cm^{-1} is due to the fluorescence lamp. The films of elemental sulphur are considered difficult to study by spectroscopic techniques (Li et al., 1993). It has been reported that vacuum electrode tends to

volatilise the sulphur above 270°K. In this case sufficient counts could be obtained to produce a good spectrum in 0.1 s of integration, considering that sulphur is a good scatter. The sharpness of the obtained peaks suggests that there are no sulphide compounds (e.g. polysulphides and sulphides) at the surface along with S^0.

In-situ experiments, providing the possibility of following the surface chemistry evolution of the minerals during anodic oxidation, could be useful to identify intermediate compounds. Several studies concerning in-situ spectroscopic experiments allowed the detection of polysulphides in the early stages of pyrite oxidation in acid solutions for a potential range of 0.6–0.7 V (SCE) (Li et al., 1993). The presence of these intermediate species has the effect of broadening the peaks, which become sharp over time. It must be pointed out that ex-situ experiments, requiring the removal of the sulphide electrode from the solution to the vacuum, can lead to one disadvantage; the loss of the electrochemical potential can modify to some extent the oxidized surface.

3.4. Analysis of electrolysis solution

Although elemental sulphur seems to be the most important oxidation product on the arsenopyrite surface for acid systems, the analysis of the solution after electrolysis revealed the presence of anionic species other than chloride, Fig. 9.

Sulphite and sulphates, which have already been detected on the electro-oxidized mineral surface by XPS, were also identified in the solution by ionic chromatography. Peaks I and II in the chromatogram correspond to the sulphate and sulphite anions, respectively. Peak III is related with the chloride ions from the leaching solution.

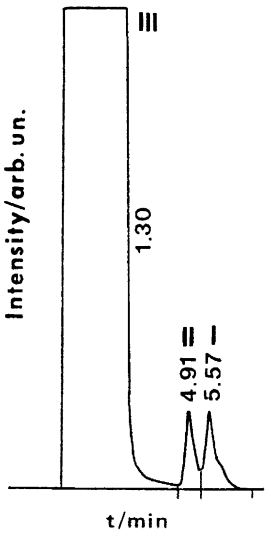

Fig. 9. Chromatogram of NaCl 1.9 M + HCl 0.1 M solution after 1 h of electro-oxidation of arsenopyrite at +0.8 V potential showing SO_4^{2-} (4.91 min; 6.70 ppm) and SO_3^{2-} (5.57 min).

The presence of iron in the solution can result from the dissolution of soluble iron oxy-sulphur species.

3.5. Electro-oxidation of the arsenopyrite concentrate

The voltammetric response of the arsenopyrite concentrate and its pure minerals suggest the occurrence of several oxidation (reduction) reactions leading to the formation of a variety of soluble and solid compounds already detected on the arsenopyrite surface by the spectroscopic study. Thus, a transformation of the sulphide matrix in which the gold is usually occluded or included can be induced by the application of a suitable anodic potential. Based on this evidence the electro-oxidation of the arsenopyrite concentrate was carried out in chloride media using an anodic potential of +0.8 V, which was selected taking into account that near this value the voltammograms of the concentrate and pure minerals show a high oxidative current. The electro-oxidized residue was subsequently submitted to thiourea leaching in order to recover the gold initially included or occluded. Thiourea leaching of the electro-reacted residue gave 90% recovery of gold, while only 21% was achieved by direct thiourea leaching of the concentrate under the same experimental conditions. The great amount of dissolved elements (iron and non-ferrous metals) in the electroleaching solution is consistent with the process efficiency. A comparison between chemical and electrochemical oxidation using chloride and sulphate solutions also proved the better performance of chloride medium and electrolytic route (Abrantes and Costa, 1996; Costa, 1996). Electro-oxidation is therefore an effective treatment for gold recovery from sulphide refractory ores. It favours metal dissolution allowing recovery of more than 90% of gold after specific leaching with acidic thiourea solution. Although elemental sulphur was the most important product of arsenopyrite oxidation — detected on the electro-oxidized surface — and although the presence of an oxidized layer mainly formed by ferric and arsenic oxides, no passivation phenomena, which can cause low gold recovery, were detected probably due to the utilization of a particulated bed anode system. Using this method, films of elemental sulphur and possible formation of metal oxides are dispersed.

4. Conclusions

The results obtained in this study show that arsenopyrite is spontaneously oxidized in the presence of air. In fact the simple exposure of the mineral to air after its polishing and before its placement in the vacuum chamber results in the formation of arsenic and iron oxides on the mineral surface. Sulphur and to a lesser extent oxy-sulphur species were also identified. After electro-oxidation in an acidic medium (+0.8 V for 1 h) the mineral surface was completely transformed mainly to elemental sulphur. The presence of other oxidized phases on the surface such as iron and arsenic oxides, as well as oxy-sulphur species, was also detected. No polysulphides were detected either in the oxidized or in the electro-oxidized surface. XPS results confirm the assumptions based on the electrochemical studies. In general our findings are broadly in agreement with

published results regarding the surface oxidation of arsenopyrite (Nesbitt et al., 1995; Richardson and Vaughan, 1989), indicating that chemical and electrochemical oxidation can essentially lead to the same oxidation products, although electro-oxidation can produce a quicker and deeper transformation of the surface. The oxidation and the electro-oxidation processes leave the surface poorer in As and Fe. In the surface overlayer, almost all Fe(II) has been oxidized to Fe (III), while As (-I) was transformed to As (III) and As (V). Sulphur that is S (-I) in arsenopyrite was mainly converted to elemental sulphur, although some higher oxidation states, such as sulphate, were found in the oxidized surfaces. As verified in previous studies (Nesbitt et al., 1995; Buckley and Walker, 1988/89) the oxidation of the three arsenopyrite components — Fe, As and S — occurs at different rates, the arsenic and iron oxidation rate being faster than the rate of sulphur oxidation. As a consequence both metals are much more affected than sulphur by oxidation and by electro-oxidation.

The success of the electrochemical treatment for the subsequent recovery of gold usually included or occluded in the arsenopyrite mineral can be explained assuming that the surface transformation is extended to the bulk and leads to the complete transformation of the sulphide mineral. Thus, with the application of electrochemical pretreatment, the sulphide matrix is transformed to elemental sulphur and to the other oxidation products detected, allowing the release of the precious metal and its accessibility to the leaching agent. When the concentrate is processed the same will occur, along with the anodic transformation of the other mineral species contained.

Importance should be given to arsenopyrite processing and tailings disposal, taking into account the high dissolution of arsenic oxidation compounds in acidic media and its toxicity.

References

Abrantes, L.M., Costa, M.C., 1996. Hydrometallurgy 40, 99–110.
Ahgelidis, T.N., Kydros, K.A., 1995. Hydrometallurgy 37, 75–88.
Ahlberg, E., Forssberg, K.S., Wang, X.H., 1990. J. Appl. Electrochem. 20, 1033–1039.
Attia, Y.A., El-Kezy, M., 1989. Hydrometallurgy 22, 219–310.
Beamson, G., Briggs, D., 1992. High resolution XPS of organic polymers. The Scienta ESCA 300 Database. Wiley, New York.
Beattie, M.J., Poling, G.W., 1987. Int. J. Miner. Process. 20, 87–108.
Bertrand, P.A., 1981. J. Vac. Sci. Technol. 18, 28–33.
Breeze, P.A., Hartnagel, H.L., Sherwood, P.M.A., 1980. J. Electrochem. Soc. 127, 454–461.
Briggs, D., Rivière, J.C., 1996. In: Briggs, D., Seah, M.P. (Eds.), Practical Surface Analysis by Auger and X-ray Photoelectron Spectroscopy, Chap. 3. Wiley, New York, pp. 85–142.
Briggs, D., Seah, M.P. (Eds.), 1996. Practical Surface Analysis by Auger and X-ray Photoelectron Spectroscopy. Wiley, New York.
Brion, D., 1980. Appl. Surf. Sci. 5, 133–152.
Bruckard, W.J., Sparrow, G.J., Woodcook, J.T., 1993. Hydrometallurgy 33, 17–41.
Buckley, A.N., Walker, G.W., 1988/1989. Appl. Surf. Sci. 35, 227–240.
Buckley, A.N., Woods, R., 1984. Aust. J. Miner. Process. 37, 2403–2413.
Chaturvedi, S., Katz, R., Guevremont, J., Schoonen, M.A.A., Strongin, D.R., 1996. Am. Mineral. 81, 261–264.
Costa, M.C., 1996. Processamento Hidrometalúrgico para Recuperação de Metais Preciosos, PhD Thesis, Faculty of Sciences of Lisbon, Portugal.

Deschênes, G., Ghali, E., Bouchet, P.L., 1998. Hydrometallurgy 47, 189–203.
Duc, C., 1992. PhD Thesis, University Henri Poincaré, Nancy 1.
Dunn, J.G., Chamberlain, A.C., 1997. Min. Eng. 10 (9), 919–928.
Dunn, J.G., Fernandez, P.G., 1987. Proceedings of the 13th International Precious Metals Conference, Canada. TMS (The Minerals, Metals & Materials Society), pp. 5–15.
Egglestbon, C.M., Ehrhardt, J.J., Stumm, W., 1996. Am. Mineral. 81, 1036–1056.
Fairthorne, G., Fornasiero, D., Ralston, J., 1997. Int. J. Miner. Process. 49, 31–48.
Fleming, C.A., 1992. Hydrometallurgy 30, 127–162.
Fornasiero, D., Li, F., Ralston, J., Smart, R.St., 1994. J. Colloid Interface Sci. 164, 333–344.
Frost, D.C., Leeder, W.R., Tapping, R.L., Wallbank, B., 1977. Fuel 56, 277–287.
Frutos, F.G., 1998. In: Gallios, G.P., Matis, K.A. (Eds.), Mineral Processing and Environment. Kluwer Academic Publishers, Dordrecht, pp. 43–72.
Fullston, D., Fornasiero, D., Ralston, J., 1999. Langmuir 15, 4530–4536.
Goode, J.R., 1993. In: Hager, J.P. (Ed.), Proceedings of 4th Extraction and Processing Division Congress, 122nd TMS Annu. Meet. TMS, Warrendale, pp. 291–317.
Griffith, W.P., White, W.B., 1975. In: Karr, C. (Ed.), Infrared and Raman Spectroscopy of Lunar and Terrestrial Minerals. Academic Press, New York, pp. 229–324.
Grunthaner, F.J., Grunthaner, P.J., Vasquez, R.P., Lewis, B.F., Maserjian, J., Madhukar, A., 1979. J. Vac. Sci. Technol. 16, 1443–1453.
Gupta, R.P., Sen, S.K., 1974. Phys. Rev. B 10, 71–79.
Hacquard, E., Bessière, J., Alnot, M., Ehrhardt, J.J., 1999. Surf. Interface Anal. 27, 849–860.
Harvey, D.T., Linton, R.W., 1981. Anal. Chem. 53, 1684–1688.
Iglesias, N., Inmaculada, P., Carranza, F., 1993. In: Hager, J.P. (Ed.), Proceedings of 4th Extraction and Processing Division Congress, 122nd TMS Annu. Meet. TMS, Warrendale, pp. 99–115.
Karthe, S., Szargan, R., Suoninen, E., 1993. Appl. Surf. Sci. 72, 157–170.
Knipe, S.W., Fleet, M.E., 1997. Can. Mineral. 35, 1485–1495.
Kontopoulos, A., Stefanakis, M., 1989. In: Jha, M.C., Hill, S.D. (Eds.), Precious Metals '89. TMS Annu. Meet., USA. TMS (The Minerals, Metals & Materials Society), pp. 179–209.
Lacoste-Bouchet, P., Deschênes, G., Ghali, E., 1998. Hydrometallurgy 47, 189–203.
Li, J., Zhu, X., Wadsworth, M.E., 1993. In: Hager, J.P. (Ed.), Proceedings of 4th Extraction and Processing Division Congress, 122nd TMS Annu. Meet. TMS, Warrendale, pp. 229–244.
Marabini, A.M., Contini, G., Cozza, C., 1993. Int. J. Miner. Process. 38, 1–20.
McCarron, J.J., Walker, G.W., Buckley, A.N., 1990. Int. J. Miner. Process. 30, 1–16.
McCliney, R.J., 1990. J. Met. 42, 10–11.
McIntyre, N.S., Zetaruk, D.G., 1977. Anal. Chem. 49 (11), 1521–1529.
Mernagh, T.P., Trudu, A.G., 1993. Chem. Geol. 103, 113–127.
Mielczarski, J.A., Cases, J.M., Alnot, M., Ehrhardt, J.J., 1996a. Langmuir 12 (10), 2519–2530.
Mielczarski, J.A., Cases, J.M., Alnot, M., Ehrhardt, J.J., 1996b. Langmuir 12 (10), 2531–2543.
Mills, P., Sullivan, J.L., 1983. J. Phys. D: Appl. Phys. 16, 723–732.
Mizokawa, Y., Iwasaki, H., Nishitani, R., Nakamura, S., 1978. J. Electron Spectrosc. Relat. Phenom. 14, 129–141.
Moulder, J.F., Stickle, W.F., Sobol, P.E., Bomben, K.D., 1992. Handbook of X-ray Photoelectron Spectroscopy, 2nd edn. Perkin-Elmer Corporation, Physical Electronics Division, Eden Prairie, Minnesota, USA.
Murthy, D.S., Prasad, P.M., 1996. Hydrometallurgy 42, 27–33.
Mycroft, J.R., Bancroft, G.M., McIntyre, N.S., Hill, I.R., 1990. J. Electroanal. Chem. 292, 139–152.
Nesbitt, H.W., Muir, I.J., 1994. Geochim. Cosmochim. Acta 59, 4667–4679.
Nesbitt, H.W., Muir, I.J., 1998. Mineral. Petrol. 62 (1–2), 123–144.
Nesbitt, H.W., Muir, I.J., Pratt, A.R., 1995. Geochim. Cosmochim. Acta 59, 1773–1786.
Paterson, C.J., 1990. In: Arbiter, N. (Ed.), Gold Advances in Precious Metals Recovery. Gordon and Breach Science Publishers, pp. 43–66.
Peters, E., 1984. In: Woods, R., Richardson, P.E., Srinivason, R. (Eds.), Electrochemistry in Minerals and Metals Processing. Electrochemical Soc. Int., pp. 343–361.
Pillai, Y., Bockris, Y., 1985. J. Colloid Interface Sci. 1, 145–153.

Prasad, M.S., Mensah-Biney, R., Pizarro, R.S., 1991. Min. Eng. 4 (12), 1257–1277.
Pratt, A.R., McIntyre, N.S., Splinter, S.J., 1998. Surf. Sci. 396, 266–272.
Pritzker, M.D., Yoon, R.H., 1988. J. Appl. Electrochem. 18, 323–332.
Richardson, S., Vaughan, D.J., 1989. Min. Mag. 53, 223–229.
Rinker, M.J., Nesbitt, H.W., Pratt, A.R., 1997. Am. Mineral. 82, 900–912.
Sanchez, V.M., Hiskey, J.B., 1991. Min. Met. Proc. 8, 1–6.
Santos, L.S., Tavares, P.F., Costa, M.C., Abrantes, L.M., 1993. Proceedings of the Symposium on the Polymetallic Sulphides on the Iberian Pyrite Belt, Apimineral, Évora, Portugal. Associação Portuguesa da Indústria Mineral (APIMINERAL) and Comitê Empresarial Português de Recursos Minerais da Faixa Piritosa Ibérica, vol. 49, pp. 1–19.
Scaini, M.J., Bancroft, G.M., Knipe, S.W., 1997. Geochim. Cosmochim. Acta 61 (6), 1223–1231.
Stec, W.J., Morgan, W.E., Albridge, R.G., Van Wazer, J.R., 1972. Inorg. Chem. 11, 219–225.
Tanuma, S., Powell, C.J., Penn, D.R., 1991. Surf. Interface Anal. 17, 927–939.
Tremblay, L., Deschênes, G., Ghali, E., McMullen, J., Lanouette, M., 1996. Int. J. Miner. Process. 48, 225–244.
Turcotte, S.B., Benner, R.E., Riley, A.M., Li, J., Wadsworth, M.E., Bodily, M.D., 1993. J. Electroanal. Chem. 347, 195–205.
Ubaldini, S., Fornari, P., Massidda, R., Abbruzzese, C., 1998. Hydrometallurgy 48, 113–124.
Vreugde, M.J., 1983. Flotation Characteristics of Arsenopyrite, PhD Thesis, University of British Columbia, Canada.
Wagner, C.D., Riggs, W.M., Davis, L.E., Moulder, J.F., Muilenberg, G.E., 1979. Handbook of X-ray Photoelectron Spectroscopy, 1st edn. Perkin-Elmer Corporation, Physical Electronics Division, Eden Prairie, Minnesota, USA.
Wagner, C.D., Bickham, D.M., 1979. NIST X-ray Photoelectron Spectroscopy Data Base.
Wang, X.H., Ahlberg, E., Forssberg, K.S., 1992. J. Appl. Electrochem. 22, 1095–1103.
Wedepohl, K.H., 1978. Handbook of Geochemistry. Springer-Verlag, Berlin.
Wiand, R., 1991. Hydrometallurgy 27, 285–296.
Woods, R., 1992. In: Murphy, O.J. (Ed.), Electrochemistry in Transaction. Plenum, New York, pp. 561–573.
Woods, R., Constable, D.C., Hamilton, I.C., et al., 1989. Int. J. Miner. Process. 27, 309–326.
Zheng, Z.M., Lin, H.K., 1994. In: Warren, G.W. (Ed.), Proceedings of 5th Extraction and Processing Division Congress, 123rd TMS Annu. Meet. TMS, San Francisco, pp. 389–406.
Zipperian, D., Raghavan, S., Wilson, J.P., 1988. Hydrometallurgy 19, 361–375.